

Phase I Study of Vismodegib in Children with Recurrent or Refractory Medulloblastoma: A Pediatric Brain Tumor Consortium Study

Amar Gajjar¹, Clinton F. Stewart², David W. Ellison³, Sue Kaste^{1,4}, Larry E. Kun⁴, Roger J. Packer⁷, Stewart Goldman⁸, Murali Chintagumpala⁹, Dana Wallace⁵, Naoko Takebe¹⁰, James M. Boyett⁵, Richard J. Gilbertson^{1,6}, and Tom Curran¹¹

Abstract

Purpose: To investigate the safety, dose-limiting toxicities, and pharmacokinetics of the smoothed inhibitor vismodegib in children with refractory or relapsed medulloblastoma.

Experimental design: Initially, vismodegib was administered daily at 85 mg/m² and escalated to 170 mg/m². The study was then revised to investigate a flat-dosing schedule of 150 mg for patients with small body surface area (BSA, 0.67–1.32 m²) or 300 mg for those who were larger (BSA, 1.33–2.20 m²). Pharmacokinetics were performed during the first course of therapy, and the right knees of all patients were imaged to monitor bone toxicity. Immunohistochemical analysis was done to identify patients with Sonic Hedgehog (SHH)-subtype medulloblastoma.

Results: Thirteen eligible patients were enrolled in the initial study: 6 received 85 mg/m² vismodegib, and 7 received 170 mg/m². Twenty eligible patients were enrolled in the flat-dosing part of the study: 10 at each dosage level. Three dose-limiting toxicities were observed, but no drug-related bone toxicity was documented. The median (range) vismodegib penetration in the cerebrospinal fluid (CSF) was 0.53 (0.26–0.78), when expressed as a ratio of the concentration of vismodegib in the CSF to that of the unbound drug in plasma. Antitumor activity was seen in 1 of 3 patients with SHH-subtype disease whose tumors were evaluable, and in none of the patients in the other subgroups.

Conclusions: Vismodegib was well tolerated in children with recurrent or refractory medulloblastoma; only two dose-limiting toxicities were observed with flat dosing. The recommended phase II study dose is 150 or 300 mg, depending on the patient's BSA. *Clin Cancer Res*; 19(22); 6305–12. ©2013 AACR.

Introduction

The Sonic Hedgehog (SHH) pathway is activated in some familial and sporadic medulloblastomas; thus, stratifying

this molecular subtype for targeted therapies may be possible (1). SHH-subtype medulloblastoma was distinguished on the basis of the presence of RNAs whose expression increases after SHH-pathway activation (2, 3). A set of mutations, primarily loss of patched-1 (PTCH1), gain-of-function in smoothed (SMO), and loss of suppressor-of-fused (SUFU), account for approximately half of SHH-medulloblastoma cases. In contrast, WNT-subtype medulloblastoma expresses target genes characteristic of the WNT-pathway activation, and most harbor activating mutations in β -catenin (4, 5). Recently, DNA-sequencing approaches identified many other, sometimes overlapping, mutations in medulloblastoma (6–9).

The first small-molecule inhibitor of the SHH pathway identified was the teratogen cyclopamine, which causes developmental abnormalities by inhibiting SMO, a membrane-associated protein that functions downstream of PTCH1 in the SHH pathway (10, 11). This led to cell-based screens for other SMO inhibitors with greater efficacy and reduced toxicity that could be developed as potential therapeutics (12, 13). The generation of a mouse model of Gorlin syndrome (14) and that of a high-incidence, early-onset model of medulloblastoma (15) permitted preclinical

Authors' Affiliations: Departments of ¹Oncology, ²Pharmaceutical Sciences, ³Pathology, ⁴Radiological Sciences, ⁵Biostatistics, and ⁶Developmental Neurobiology, St Jude Children's Research Hospital, Memphis, Tennessee; ⁷Center for Neuroscience Research, Children's National Medical Center, Washington, DC; ⁸Division of Hematology–Oncology, Ann & Robert H. Lurie Children's Hospital of Chicago, Chicago, Illinois; ⁹Department of Pediatrics, Texas Children's Hospital, Houston, Texas; ¹⁰Investigational Drug Branch, Cancer Therapy Evaluation Program, National Cancer Institute, Bethesda, Maryland; and ¹¹Department of Pathology and Laboratory Medicine, Children's Hospital of Philadelphia, Philadelphia, Pennsylvania

Note: Supplementary data for this article are available at Clinical Cancer Research Online (<http://clincancerres.aacrjournals.org/>).

Prior presentation: This work was presented, in part at the 46th Annual Meeting of the American Society of Clinical Oncology, June 4–8, 2010, Chicago, IL.

Corresponding Author: Amar Gajjar, Department of Oncology, MS 260, St Jude Children's Research Hospital, 262 Danny Thomas Place, Memphis TN 38105. Phone: 901-595-2615; Fax: 901-521-9005; E mail: amar.gajjar@stjude.org

doi: 10.1158/1078-0432.CCR-13-1425

©2013 American Association for Cancer Research.

Translational Relevance

The smoothed inhibitor vismodegib has antitumor activity in adults. However, its effects in children have not been thoroughly assessed, and preclinical results suggest that the drug may cause growth defects in bone and teeth. In this phase I study, we examined the safety, efficacy, toxicity, and pharmacokinetics of vismodegib in pediatric patients with recurrent medulloblastoma. Molecular heterogeneity within the SHH medulloblastoma subtype—namely *GLI* or *MYCN* amplifications or *SUFU*, *MLL2*, *P53*, and *SMO* mutations—may have resulted in the observed variable efficacy of vismodegib. We detected no deleterious effects on bone growth. Ongoing phase II studies of recurrent SHH medulloblastoma in adults and children will further elucidate the efficacy and chronic toxicity of vismodegib.

studies that demonstrated remarkable efficacy of the tool compound HhAntag (16). These findings stimulated further medicinal chemistry, leading to the first-in-class compound GDC-0449 (vismodegib; ref. 17) that was entered into advanced solid tumor clinical trials (18). Several *SMO* inhibitors are currently being tested in the phase I and II settings against various tumor types (1, 19).

In a phase I trial of vismodegib for advanced, metastatic solid tumors, patients with basal cell carcinoma (BCC) showed a 60% response rate (18). The only other response, albeit transient and incomplete, occurred in a patient with metastatic medulloblastoma (20). The common feature of these tumors is the presence of activating mutations in the SHH pathway (1). The metastatic medulloblastoma eventually relapsed due to a *SMO* mutation that abrogated vismodegib binding (21). On the basis of these data, we designed a phase I trial to determine the toxicity, pharmacokinetics, and recommended phase II dosage of vismodegib in pediatric patients with refractory or recurrent medulloblastoma. In light of preclinical data indicating that *SMO* inhibitors cause growth defects in the bones and teeth of mice (22, 23), this trial was designed to detect developmental toxicities that are unique to children.

Patients and Methods

Patients

Eligible patients were 3 to 21 years of age, had a histologically verified diagnosis of medulloblastoma that was recurrent, progressive, or refractory to standard therapy, and had a Karnofsky or Lansky score of 60 or higher documented within 2 weeks of registration. The initial trial required a body surface area (BSA) that was no more than 2.0 m²; the flat-dosing trial required that BSA be 0.67 to 2.5 m². Patients were eligible if they had stable neurologic deficits for at least 1 week before enrolling, had recovered from previous treatment-related toxicity, and had not received any of the following treatments during the given period before study

entry: growth factors within 1 week, myelosuppressive chemotherapy or immunotherapy within 4 weeks (6 weeks if nitrosourea), craniospinal irradiation within 3 months, local radiotherapy to the primary tumor within 8 weeks, or focal irradiation for symptomatic metastatic sites within 2 weeks.

Pregnant patients and those with clinically significant, unrelated systemic illness were excluded. Patients were not allowed to take any other anticancer or investigational drug while on the study. Other requirements included adequate functioning of bone marrow (peripheral ANC $\geq 1,000/\mu\text{L}$, platelet count $\geq 100,000/\mu\text{L}$, and transfusion-independent hemoglobin ≥ 8.0 g/dL), kidneys (serum creatinine $\leq 1.5 \times$ upper-normal limit [UNL] for age or GFR ≥ 70 mL/min per 1.73 m²), and liver (total bilirubin $\leq 1.5 \times$ institutional UNL for age, ALT and AST, $\leq 2.5 \times$ institutional UNL for age, and albumin ≥ 2.5 g/dL). All patients with child-bearing potential were required to use two forms of contraception, including one barrier method, during their participation in the study and for 12 months thereafter. Informed consent was obtained from patients, parents, or guardians; assent was obtained, as appropriate, at the time of enrollment. The institutional review boards of each Pediatric Brain Tumor Consortium (PBTC) institution approved the protocol before patient enrollment, and continuing approval was maintained throughout the study. All data were managed as per the Health Insurance Portability and Accountability Act of 1996.

Study design

Vismodegib was supplied by Genentech and distributed by the National Cancer Institute (NCI) Cancer Therapy Evaluation Program. Initially, Genentech produced vismodegib as 25 and 150 mg capsules. In the initial study, two dosages were used: 85 and 170 mg/m² (rounded to the nearest 25 mg), and each course was 28 days long. Genentech then ceased to manufacture the 25-mg capsule, so we revised the protocol. In the second study, a flat-dosing schema was used: smaller patients (BSA, 0.67–1.32 m²) received 150 mg/day, and larger patients (BSA, 1.33–2.2 m²) received 300 mg/day.

The original PBTC025 (NCT00822458) study was designed to determine a dosage for the subsequent phase II trial based on a comparison of the 95% confidence interval estimated for the day 21 mean steady-state concentration (C_{ss}) of total vismodegib (protein-bound and unbound) in plasma of each cohort, provided that both dosages were safe. Once the 25 mg capsules were no longer available, the recommended BSA-adjusted dosages were not identical to their assigned dosages, and large deviations from the targeted level of 170 mg/m² were unavoidable (Fig. 1). Our flat-dosing strategy (Supplementary Table S1) was devised to minimize this deviation. Patients could receive as many as 26 courses in the absence of disease progression.

Dose-limiting toxicity (DLT) was defined as any of the following events that were at least possibly related to the study drug and occurred during the first 28 days on study.

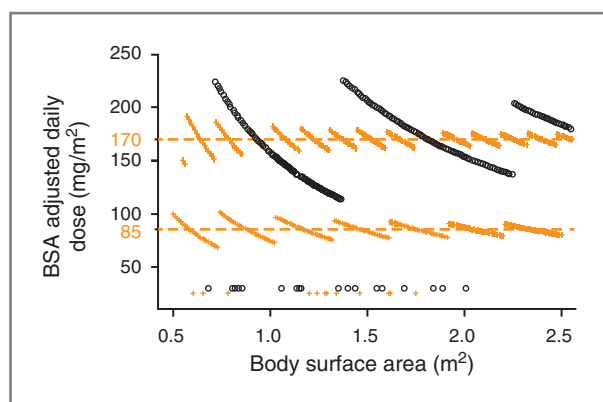


Figure 1. Variations in target dosages of vismodegib reflect interpatient differences in body surface area (BSA). Deliverable doses vary from targeted doses due to BSA-based dosing and limited drug formulation. Orange symbols (+) represent the initial cohort who received 25-mg capsules, and the black symbols (○) represent the flat-dosing cohort who received 150-mg capsules. Dosing strategy was based on minimizing the difference between the deliverable and targeted doses. Variation from the targeted doses was substantially less in the initial study than in the flat-dosing trial due to the initial availability of the 25-mg capsules. With a targeted dose of 170 mg/m² in the flat-dosing cohort, BSA ranges were chosen to minimize the difference between the targeted and the deliverable doses. Individual patient BSAs are plotted just above the x-axis.

Hematologic DLT was defined as grade 4 neutropenia and thrombocytopenia, or grade 3 thrombocytopenia requiring transfusions on more than two occasions during a treatment course. Nonhematologic DLT was defined as any grade 4 nonhematologic toxicity attributable to vismodegib treatment and most grade 3 nonhematologic toxicities, excluding the following conditions: grade 3 nausea and vomiting for 5 days or less despite treatment with appropriate antiemetics, grade 3 ALT or AST that returns to levels that meet eligibility criteria within 5 days of vismodegib interruption and do not recur upon rechallenge, grade 3 fever or infection for no more than 5 days, grade 3 hypophosphatemia, hypokalemia, hyponatremia, or hypomagnesemia responsive to oral supplementation. DLTs were graded according to the NCI Common Terminology Criteria for Adverse Events (version 4.0).

Pretreatment evaluations included a history, physical examination, dental evaluation, knee MRI, performance status, disease evaluation, complete blood count (CBC), electrolyte measurement, renal and liver function tests, and pregnancy tests for female patients of childbearing age. CBC, electrolytes, and renal and liver functions were tested weekly during the first course and monthly before starting subsequent courses. History and physical examination were obtained before each course. Disease evaluations, dental evaluation, and MRIs of the knee were performed every 3 months and at the end of therapy. Contraceptive methods were confirmed and documented, and the teratogenic potential of vismodegib was explained before each course.

Tumor responses were defined as follows: Complete response—no measurable lesions on MRI. If disease was detected in the cerebrospinal fluid (CSF) before treatment,

the CSF must be negative. Partial response—at least 50% reduction in tumor area compared with baseline measurements. Stable disease—MRI features that do not meet the criteria for partial response or progressive disease. Progressive disease—more than 25% increase in tumor area compared with the smallest area measured since protocol therapy initiation or the detection of a new lesion. Patients whose disease response was based on imaging received a stable or decreasing dose of corticosteroids, had to show improved neurologic function, and the response had to be maintained for at least 8 weeks.

Pharmacokinetics

Mandatory pharmacokinetics were conducted in all patients, beginning on day 1 of the first course: blood samples were collected before the first vismodegib dose and at 2, 8, 24, 48, 72, and either 96, 120, or 144 hours thereafter. Vismodegib was withheld on days 2 and 3 to obtain samples for pharmacokinetic analysis. In addition, blood samples were obtained prior to the vismodegib dose on days 14 and 21 of the first course. Blood samples were centrifuged, and the plasma was stored at -80°C until the total- and unbound-drug concentrations were analyzed by high-performance liquid chromatography with tandem mass spectrometry (24). Plasma samples were prepared for unbound-drug analysis using a 96-well equilibrium dialyzer (Harvard Apparatus). Pharmacokinetics of total and unbound drug consisted of time to maximum plasma concentration (T_{max}) and maximum plasma concentration (C_{max}) on day 1, area under the concentration-time curve ($\text{AUC}_{0\rightarrow 72}$), and the C_{ss} which was obtained prior to the dose on day 21 (i.e., C_{ss} trough). Apparent oral clearance was estimated using standard, noncompartmental methods. Consenting patients with ventricular-access devices provided simultaneous ventricular CSF and plasma samples at 1, 3, and 8 hours after the first vismodegib dose. CSF vismodegib concentrations were analyzed via the same method as plasma vismodegib concentrations (24). The ratio of vismodegib $\text{AUC}_{0\rightarrow 8}$ in CSF to that in plasma (total or unbound) was used as a measure of drug penetration.

Immunohistochemistry

Immunohistochemical analysis (IHC) was performed according to established protocols with antibodies against GFAP (M0761; 1:250; Dako), synaptophysin (NCL-L-Synap-299; 1:400; Leica Microsystems), NEU-N (MAB377; 1:10,000; Chemicon), p27^{Kip1} (M7203; 1:50; Dako), and Ki-67 (M7240; 1:200; Dako). Molecular subgroups of disease (SHH, WNT, and non-SHH/WNT) were disclosed using four antibodies, as described previously (25).

MRI

A noncontrast MRI of the right knee was obtained within 4 weeks of starting therapy, every 3 months thereafter, and at the end of therapy to assess drug-related bone toxicity. The following MRI sequences were used: coronal fat-saturated T₁ spin echo, sagittal fat-saturated proton density, and three-dimensional (3D) double-echo steady state.

Table 1. Characteristics of patients with medulloblastoma in a phase I trial of vismodegib

Characteristic	Initial cohort (n = 13)	Flat-dosing cohort (n = 20)
Sex ratio (male:female)	10:3	15:5
Age at study entry, y		
Median	11.6	14.5
Range	4.4–21	3.9–20.3
Histologic features		
Classic	6	8
Desmoplastic/nodular	0	2
Anaplastic	3	4
Large cell	0	1
Not specified	3	2
Inadequate tumor sample	1	3
Prior therapy		
Chemotherapy and RT	13	18
Chemotherapy, RT, and BMT	0	2
No. of courses of vismodegib		
Median	2	1.5
Range	1–26	1–8

Abbreviations: BMT, bone marrow transplantation; RT, radiotherapy.

Results

Patient characteristics

Of the 34 patients who enrolled, 33 met the eligibility criteria (Table 1). Thirteen patients participated in the initial cohort, and 20 in the flat-dosing cohort. The median number of courses administered was two (range, 1–26).

Toxicity

Twenty-seven of 33 (81.8%) patients were evaluable for DLT (Table 2). A list of adverse events and toxicities that occurred in more than 20% of the patients is provided (Supplementary Table S2). Of the 6 patients who were not evaluable, 5 experienced progressive disease during the first course, and 1 withdrew from the study. No drug-related dental abnormalities were observed.

MRI

Thirty-three patients underwent 72 MRIs of their knees. All studies were centrally reviewed; 1 was deemed nonanalyzable. Thirteen patients underwent one study, and 20 completed multiple studies (range, 2–10 studies). The median MRI follow-up was 8 months (range, 0.5–26 months). At baseline, 23 patients were classified as Laor grade 1 (immature skeletal stage); 3 as Laor grade 2; 5 as Laor grade 3; 1 as Laor grade 4; and 1 patient lacked baseline information (26).

At the time of initial MRI, femoral cartilaginous clefts were identified in 6 patients; two developed after study enrollment. Tibial cartilaginous clefts were noted in 3 patients; two were present at study entry, and one was transient. Femoral bone bridges were noted in 4 patients: two were present at study entry, and two developed during follow-up at 2 and 13 months, respectively. Tibial bone bridges were noted in 5 patients: three were present at study entry, and two were seen on follow-up MRIs. Focal physal thickening was present in 2 patients at study entry; one had the appearance of possible prior trauma. Focal femoral physal thickness increased by 2 mm medially in 1 patient.

Additional baseline findings were as follows. Six patients had femoral osteonecrosis in the following regions: epiphyseal ($n = 4$), metaphyseal ($n = 3$), and diaphyseal ($n = 3$). Four patients also had tibial osteonecrosis in the same regions: epiphyseal ($n = 2$), metaphyseal ($n = 1$), and diaphyseal ($n = 1$). Four patients had nonossifying fibromas (2 were present at study entry; 1 showed evidence of healing; and 1 progressed over time). One patient had widespread metastatic disease at baseline. Six patients had increased joint fluid, which was present in 3 patients at study entry. Two patients had intraarticular inflammation, which was present in 1 patient at study entry.

Pharmacokinetics

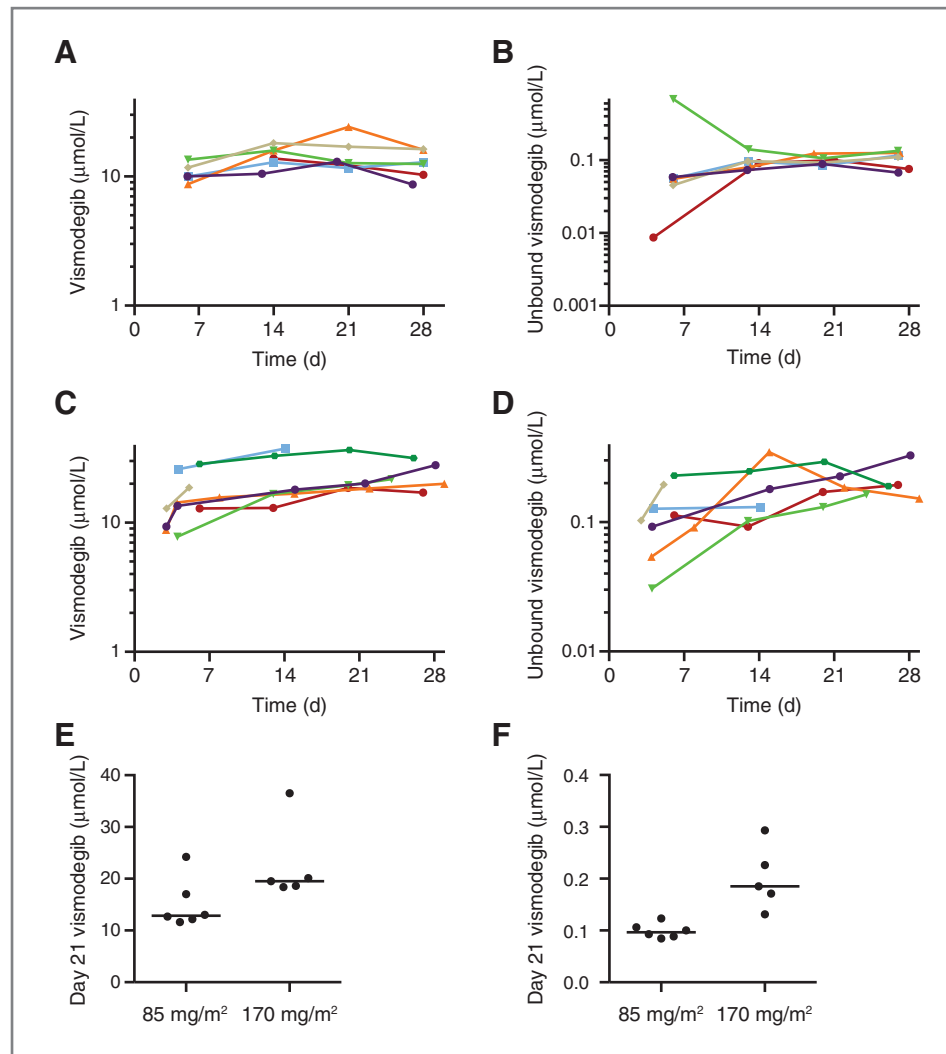
Serial plasma samples were collected from all patients. Day 21 vismodegib C_{ss} differed between the two initial dosage groups (Fig. 2E and F). The vismodegib AUC_{0-72} data are provided (Supplementary Fig. S1), as are the pharmacokinetics for total vismodegib (Table 3) and unbound vismodegib (Supplementary Table S3).

In the CSF samples available from 3 patients, the median (range) of drug penetration was 0.0026 (0.0014–0.0062), when expressed as a ratio of CSF vismodegib to the total

Table 2. Dose-limiting toxicity of vismodegib in patients with medulloblastoma

Cohort/dose	No. patients enrolled	No. patients evaluable for DLT	No. patients with DLT	DLT
Initial cohort				
85 mg/m ²	6	6	0	
170 mg/m ²	7	6	1	Grade-3 γ -glutamyl transferase
Flat-dosing cohort				
150 mg	10	8	1	Grade-4 hypokalemia
300 mg	10	7	1	Grade-3 thrombocytopenia

Figure 2. Pharmacokinetics of vismodegib after a 28-day administration of 85 or 170 mg/m². Plasma concentrations of total vismodegib after 85 mg/m² (A) or 170 mg/m² (C) and unbound vismodegib after 85 mg/m² (B) or 170 mg/m² (D) are shown for each patient. E, the medians and scatter of steady-state plasma concentration (C_{ss}) were also measured on day 21. The total vismodegib C_{ss} (E) and unbound vismodegib C_{ss} (F) significantly differed between the two groups (Mann–Whitney; *P* = 0.026 and *P* = 0.022, respectively).



concentration in plasma and 0.53 (0.26–0.78), when expressed as a ratio of CSF vismodegib to that of unbound drug in plasma. Total vismodegib plasma concentrations were correlated with α -1-acid glycoprotein (AAGP) concentrations measured in the same sample ($R^2 = 0.38$; Supplementary Fig. S2).

Identification of SHH-subtype medulloblastoma

Four patients had inadequate tissue available to determine their medulloblastoma subtype. Analysis of the 29 tissue samples identified SHH ($n = 7$), WNT ($n = 1$), and non-SHH/WNT ($n = 21$) medulloblastomas (Fig. 3). Classic, anaplastic, and large-cell histologic features were found in WNT and non-SHH/WNT medulloblastomas (25). Nodular desmoplastic histology was present only in the SHH subgroup.

Tumor response

Of the 7 patients with SHH medulloblastoma, 3 had evaluable disease and were treated with the recommended

phase II study dosage. One patient had a complete response, which was not sustained for 8 weeks; the other 2 experienced no response. Their durations of therapy were 22, 25, and 168 days, respectively. Of the remaining patients with SHH medulloblastoma, 3 had evaluable disease and were treated in the initial cohort for 7, 52, and 500 days, respectively. One patient with SHH-subtype did not have evaluable disease and was on therapy for 92 days. None of the 13 patients in the other medulloblastoma subgroups who were evaluable and treated with the phase II study dosage responded; their median duration of therapy was 41 days (range, 6–217 days).

Discussion

Targeted anticancer therapies induce remission or prolong stabilization of disease with less toxicity than conventional chemotherapy (27, 28). *PTCH* mutations leading to constitutive activation of the SHH pathway are present in a subgroup of SHH medulloblastoma (7). Agents that specifically

Table 3. Pharmacokinetics of total plasma vismodegib in pediatric patients with medulloblastoma

Dose	No. of patients	Actual dosage (mg/m ² /d)	Pharmacokinetic parameters median (range)				
			<i>T</i> _{max} (h)	<i>C</i> _{max} ^a (μmol/L)	AUC _{0–72} (μmol/L·h)	<i>C</i> _{ss} ^b (μmol/L)	CL/F (L/h/m ²)
85 mg/m ² /d	6	80 (77–92)	59.8 (8.2–75.7)	6.3 (1.9–10.2)	394 (134–564)	12.9 (11.6–24.2)	0.62 (0.38–0.67)
170 mg/m ² /d	7	163 (154–170)	8.1 (1.0–74.4)	10.4 (4.9–20.9)	660 (255–1336)	19.5 (18.4–36.5)	0.83 (0.44–0.86)
150 mg/d	10	158 (130–221)	23.5 (1.9–75.0)	8.8 (4.8–27.2)	501 (315–1644)	16.8 (12.5–38.4)	0.84 (0.48–1.43)
300 mg/d	9	183 (149–222)	37.3 (2.1–71.7)	7.0 (2.1–22.0)	460 (77–1022)	24.4 (11.4–41.9)	0.77 (0.42–1.38)

Abbreviations: AUC_{0–72}, area under the plasma concentration–time curve during the first 72 hours after administration; CL/F, apparent oral clearance of total drug from plasma; *C*_{max}, maximum drug concentration in plasma; *C*_{ss}, steady-state concentration of drug in plasma; *T*_{max}, time to reach maximum drug concentration in plasma after administration.

^a*C*_{max} was measured on day 1 of vismodegib course.

^b*C*_{ss} was measured on day 21 of vismodegib course.

block downstream signaling of this pathway could regress tumors, thereby resulting in a novel approach to treat this SHH subtype (29). Such therapy could ameliorate the late toxicities of current treatments that use craniospinal irradiation in conjunction with cytotoxic chemotherapy (30).

An adult phase I study of vismodegib, which included 33 patients with BCC and 1 with medulloblastoma, used 3 dosage levels: 150, 270, and 540 mg/day. Six patients experienced grade 4 toxicity, and 19 experienced grade 3 events most commonly involving hyponatremia, fatigue, and abdominal pain. The recommended phase II dosage was 150 mg/d; tumor responses were seen in 19 patients with BCC and in the patient with medulloblastoma (unconfirmed). The investigators demonstrated *GLI1* downmodu-

lation in noninvolved skin, and concluded that vismodegib had an acceptable safety profile and encouraging antitumor activity in BCC (31, 32). A subsequent multicenter, two-cohort, nonrandomized phase II study enrolled patients with metastatic or locally advanced BCC. The response rates of the two cohorts were 30% and 43%. Adverse events occurred in more than 30% of patients, and serious adverse events occurred in 25%; grade 3 or 4 adverse events included muscle spasms, weight loss, fatigue, and loss of appetite (33).

Here, we showed that treatment with vismodegib is safe and feasible in pediatric patients. Only 3 patients experienced DLTs. Despite the preclinical model's prediction of bone and dental toxicity, neither was detected. Several patients were exposed to steroids during the perioperative

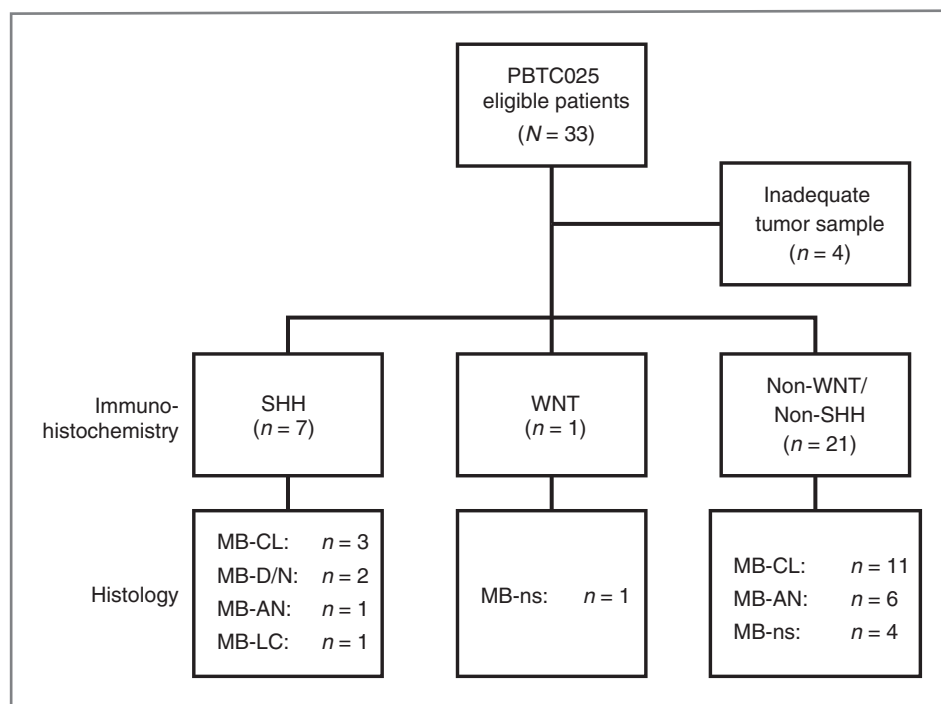


Figure 3. Diagram of medulloblastoma characteristics, as determined by immunohistochemical and histologic analyses. Immunohistochemical analysis grouped samples as SHH, WNT, or non-SHH/WNT tumors. Histologic categories included anaplastic (AN), classic (CL), desmoplastic nodular (D/N), large-cell (LC), or nonspecified (ns) tumors.

period, and baseline MRIs showed osteonecrotic changes due to prior therapy. We will continue to document the effects of prolonged exposure to vismodegib in our ongoing phase II studies.

The pharmacokinetics of vismodegib in children is comparable with that in adults. In our study, vismodegib had a unique oral absorption characterized by little decline in the plasma concentrations over 72 hours after a single dose. A recent study by Graham and colleagues showed that the primary determinants of vismodegib disposition in adults include solubility-limited absorption after oral administration, limited metabolic elimination, and interactions with AAGP (34). We also observed a relationship between AAGP and total plasma vismodegib concentrations. Unlike what was observed in adults, the vismodegib systemic exposure in pediatric patients, whether measured by AUC_{0-72} , C_{max} , or day 21 C_{ss} , was higher in those who received the 170 mg/m² dosage. Wong and colleagues conducted preclinical pharmacokinetic/pharmacodynamic studies of vismodegib and set a target unbound concentration in plasma (0.042–0.068 μmol/L) to meet or exceed the free IC₉₅ for *GLII* inhibition and ensure maximal clinical benefit (35). At day 21, the median concentration in each of our dosage groups exceeded that target; with a CSF penetration of 0.53, CSF vismodegib concentrations probably did as well. However, we observed substantial interpatient variability in all aspects of vismodegib disposition, including CSF penetration.

Prospectively selecting patients for targeted therapies is a challenge, especially patients with CNS tumors. The most accurate method to classify tumors is RNA-expression profiling, yet fresh tumor samples are not always available at diagnosis or relapse. We used IHC to detect proteins encoded by genes that would be expressed based on the RNA-expression data. IHC is a robust approach to distinguishing WNT and SHH medulloblastomas, but it cannot reliably distinguish Groups 3 and 4, which we pooled as non-SHH/WNT subtype (25). Further confirmation by other methods is required in prospective studies (3). The ideal method would be one that uses fixed tissues to ensure the inclusion of all patients.

Vismodegib demonstrated antitumor activity in 1 patient with SHH medulloblastoma and evaluable disease treated with the phase II dosage. This finding is consistent with responses seen in adults with BCC and a single case of an adult with metastatic medulloblastoma outside the CNS (18, 20). The mechanism of resistance was an acquired mutation in the *SMO* receptor that prevented binding of vismodegib (21). The lack of tumor tissue at the time of disease progression prevented us from studying the mechanism of resistance in our patients. Rapidly evolving data

from recent whole-genome-sequencing studies suggest molecular heterogeneity within SHH medulloblastoma: *GLI* or *MYCN* amplifications or *SUFU*, *MLL2*, *P53*, and *SMO* mutations could explain the lack of efficacy seen with vismodegib in all SHH medulloblastomas (7–9, 36).

Our data demonstrate the safety, feasibility, pharmacokinetics, and early efficacy of vismodegib in pediatric patients with recurrent medulloblastoma. Ongoing phase II studies of recurrent SHH medulloblastoma in adults and children will further elucidate the efficacy and chronic toxicity of vismodegib. Further understanding of the biology of SHH medulloblastoma may justify combination of *SMO* antagonists with conventional chemotherapy or other targeted agents in future clinical protocols.

Disclosure of Potential Conflicts of Interest

D.W. Ellison has ownership interests, including patents. S. Goldman has a consultant/Advisory Board relationship with Novartis. T. Curran has a consultant/Advisory Board relationship with Redx Pharma Ltd. No potential conflicts of interest were disclosed by the other authors.

Authors' Contributions

Conception and design: A. Gajjar, C.F. Stewart, D.W. Ellison, L.E. Kun, R. Packer, N. Takebe, J.M. Boyett, T. Curran

Development of methodology: A. Gajjar, C.F. Stewart, D.W. Ellison, S.C. Kaste, T. Curran

Acquisition of data (provided animals, acquired and managed patients, provided facilities, etc.): C.F. Stewart, D.W. Ellison, S.C. Kaste, R. Packer, S. Goldman, M. Chintagumpala, N. Takebe

Analysis and interpretation of data (e.g., statistical analysis, biostatistics, computational analysis): A. Gajjar, C.F. Stewart, D.W. Ellison, S.C. Kaste, R. Packer, D. Wallace, N. Takebe, J.M. Boyett, T. Curran

Writing, review, and/or revision of the manuscript: A. Gajjar, C.F. Stewart, D.W. Ellison, S.C. Kaste, L.E. Kun, R. Packer, S. Goldman, M. Chintagumpala, D. Wallace, N. Takebe, J.M. Boyett, R.J. Gilbertson, T. Curran

Administrative, technical, or material support (i.e., reporting or organizing data, constructing databases): A. Gajjar, D.W. Ellison, L.E. Kun, N. Takebe, J.M. Boyett

Study supervision: A. Gajjar, L.E. Kun, N. Takebe

Acknowledgments

The authors thank Angela McArthur for editing the manuscript and Arzu Onar-Thomas for developing the dosing strategy.

Grant Support

This work was supported, in part, by the National Institutes of Health (grant no. U01 CA 81457 to the Pediatric Brain Tumor Consortium; grant no. P01 CA 096832 to T. Curran and R. Gilbertson), the Cancer Center CORE (grant no. CA 21765), the Noyes Brain Tumor Foundation, Musicians Against Childhood Cancer (MACC), and the America Lebanese Syrian Associated Charities (ALSAC).

The costs of publication of this article were defrayed in part by the payment of page charges. This article must therefore be hereby marked *advertisement* in accordance with 18 U.S.C. Section 1734 solely to indicate this fact.

Received May 23, 2013; revised September 5, 2013; accepted September 8, 2013; published OnlineFirst September 27, 2013.

References

- Ng JM, Curran T. The Hedgehog's tale: developing strategies for targeting cancer. *Nat Rev Cancer* 2011;11:493–501.
- Pomeroy SL, Tamayo P, Gaasenbeek M, Sturla LM, Angelo M, McLaughlin ME, et al. Prediction of central nervous system embryonal tumour outcome based on gene expression. *Nature* 2002;415:436–42.
- Northcott PA, Shih DJ, Remke M, Cho YJ, Kool M, Hawkins C, et al. Rapid, reliable, and reproducible molecular sub-grouping of clinical medulloblastoma samples. *Acta Neuropathol* 2012;123:615–26.
- Thompson MC, Fuller C, Hogg TL, Dalton J, Finkelstein D, Lau CC, et al. Genomics identifies medulloblastoma subgroups that are

- enriched for specific genetic alterations. *J Clin Oncol* 2006;24:1924–31.
5. Northcott PA, Korshunov A, Witt H, Hielscher T, Eberhart CG, Mack S, et al. Medulloblastoma comprises four distinct molecular variants. *J Clin Oncol* 2011;29:1408–14.
 6. Parsons DW, Li M, Zhang X, Jones S, Leary RJ, Lin JC, et al. The genetic landscape of the childhood cancer medulloblastoma. *Science* 2011;331:435–9.
 7. Robinson G, Parker M, Kranenburg TA, Lu C, Chen X, Ding L, et al. Novel mutations target distinct subgroups of medulloblastoma. *Nature* 2012;488:43–8.
 8. Jones DT, Jager N, Kool M, Zichner T, Hutter B, Sultan M, et al. Dissecting the genomic complexity underlying medulloblastoma. *Nature* 2012;488:100–5.
 9. Pugh TJ, Weeraratne SD, Archer TC, Pomeranz Krummel DA, Auclair D, Bochicchio J, et al. Medulloblastoma exome sequencing uncovers subtype-specific somatic mutations. *Nature* 2012;488:106–10.
 10. Cooper MK, Porter JA, Young KE, Beachy PA. Teratogen-mediated inhibition of target tissue response to Shh signaling. *Science* 1998;280:1603–7.
 11. Chen JK, Taipale J, Cooper MK, Beachy PA. Inhibition of Hedgehog signaling by direct binding of cyclopamine to Smoothened. *Genes Dev* 2002;16:2743–8.
 12. Frank-Kamenetsky M, Zhang XM, Bottega S, Guicherit O, Wichterle H, Dudek H, et al. Small-molecule modulators of Hedgehog signaling: identification and characterization of Smoothened agonists and antagonists. *J Biol* 2002;1:10.
 13. Mas C, Ruiz i Altaba A. Small molecule modulation of HH-Gli signaling: current leads, trials and tribulations. *Biochem Pharmacol* 2010;80:712–23.
 14. Goodrich LV, Milenkovic L, Higgins KM, Scott MP. Altered neural cell fates and medulloblastoma in mouse patched mutants. *Science* 1997;277:1109–13.
 15. Wetmore C, Eberhart DE, Curran T. Loss of p53 but not ARF accelerates medulloblastoma in mice heterozygous for patched. *Cancer Res* 2001;61:513–6.
 16. Romer JT, Kimura H, Magdaleno S, Sasai K, Fuller C, Baines H, et al. Suppression of the Shh pathway using a small molecule inhibitor eliminates medulloblastoma in Ptc1(+/-)p53(-/-) mice. *Cancer Cell* 2004;6:229–40.
 17. Robarge KD, Brunton SA, Castaneda GM, Cui Y, Dina MS, Goldsmith R, et al. GDC-0449—a potent inhibitor of the hedgehog pathway. *Bioorg Med Chem Lett* 2009;19:5576–81.
 18. Von Hoff DD, LoRusso PM, Rudin CM, Reddy JC, Yauch RL, Tibes R, et al. Inhibition of the hedgehog pathway in advanced basal-cell carcinoma. *N Engl J Med* 2009;361:1164–72.
 19. Low JA, de Sauvage FJ. Clinical experience with Hedgehog pathway inhibitors. *J Clin Oncol* 2010;28:5321–6.
 20. Rudin CM, Hann CL, Lattera J, Yauch RL, Callahan CA, Fu L, et al. Treatment of medulloblastoma with hedgehog pathway inhibitor GDC-0449. *N Engl J Med* 2009;361:1173–8.
 21. Yauch RL, Dijkgraaf GJ, Alicke B, Januario T, Ahn CP, Holcomb T, et al. Smoothened mutation confers resistance to a Hedgehog pathway inhibitor in medulloblastoma. *Science* 2009;326:572–4.
 22. Kimura H, Ng JM, Curran T. Transient inhibition of the Hedgehog pathway in young mice causes permanent defects in bone structure. *Cancer Cell* 2008;13:249–60.
 23. Seidel K, Ahn CP, Lyons D, Nee A, Ting K, Brownell I, et al. Hedgehog signaling regulates the generation of ameloblast progenitors in the continuously growing mouse incisor. *Development* 2010;137:3753–61.
 24. Ding X, Chou B, Graham RA, Cheeti S, Percey S, Matassa LC, et al. Determination of GDC-0449, a small-molecule inhibitor of the Hedgehog signaling pathway, in human plasma by solid phase extraction-liquid chromatographic-tandem mass spectrometry. *J Chromatogr B Analyt Technol Biomed Life Sci* 2010;878:785–90.
 25. Ellison DW, Dalton J, Kocak M, Nicholson SL, Fraga C, Neale G, et al. Medulloblastoma: clinicopathological correlates of SHH, WNT, and non-SHH/WNT molecular subgroups. *Acta Neuropathol* 2011;121:381–96.
 26. Laor T, Chun GF, Dardzinski BJ, Bean JA, Witte DP. Posterior distal femoral and proximal tibial metaphyseal stripes at MR imaging in children and young adults. *Radiology* 2002;224:669–74.
 27. Zhang J, Yang PL, Gray NS. Targeting cancer with small molecule kinase inhibitors. *Nat Rev Cancer* 2009;9:28–39.
 28. Janne PA, Gray N, Settleman J. Factors underlying sensitivity of cancers to small-molecule kinase inhibitors. *Nat Rev Drug Discov* 2009;8:709–23.
 29. Rubin LL, de Sauvage FJ. Targeting the Hedgehog pathway in cancer. *Nat Rev Drug Discov* 2006;5:1026–33.
 30. Mulhern RK, Merchant TE, Gajjar A, Reddick WE, Kun LE. Late neurocognitive sequelae in survivors of brain tumours in childhood. *Lancet Oncol* 2004;5:399–408.
 31. LoRusso PM, Rudin CM, Reddy JC, Tibes R, Weiss GJ, Borad MJ, et al. Phase I trial of hedgehog pathway inhibitor vismodegib (GDC-0449) in patients with refractory, locally advanced or metastatic solid tumors. *Clin Cancer Res* 2011;17:2502–11.
 32. LoRusso PM, Jimeno A, Dy G, Adjei A, Berlin J, Leichman L, et al. Pharmacokinetic dose-scheduling study of hedgehog pathway inhibitor vismodegib (GDC-0449) in patients with locally advanced or metastatic solid tumors. *Clin Cancer Res* 2011;17:5774–82.
 33. Sekulic A, Migden MR, Oro AE, Dirix L, Lewis KD, Hainsworth JD, et al. Efficacy and safety of vismodegib in advanced basal-cell carcinoma. *N Engl J Med* 2012;366:2171–9.
 34. Graham RA, Lum BL, Cheeti S, Jin JY, Jorga K, Von Hoff DD, et al. Pharmacokinetics of hedgehog pathway inhibitor vismodegib (GDC-0449) in patients with locally advanced or metastatic solid tumors: the role of alpha-1-acid glycoprotein binding. *Clin Cancer Res* 2011;17:2512–20.
 35. Wong H, Alicke B, West KA, Pacheco P, La H, Januario T, et al. Pharmacokinetic-pharmacodynamic analysis of vismodegib in pre-clinical models of mutational and ligand-dependent Hedgehog pathway activation. *Clin Cancer Res* 2011;17:4682–92.
 36. Northcott PA, Shih DJ, Peacock J, Garzia L, Morrissy AS, Zichner T, et al. Subgroup-specific structural variation across 1,000 medulloblastoma genomes. *Nature* 2012;488:49–56.

Clinical Cancer Research

Phase I Study of Vismodegib in Children with Recurrent or Refractory Medulloblastoma: A Pediatric Brain Tumor Consortium Study

Amar Gajjar, Clinton F. Stewart, David W. Ellison, et al.

Clin Cancer Res 2013;19:6305-6312. Published OnlineFirst September 27, 2013.

Updated version Access the most recent version of this article at:
doi:[10.1158/1078-0432.CCR-13-1425](https://doi.org/10.1158/1078-0432.CCR-13-1425)

Supplementary Material Access the most recent supplemental material at:
<http://clincancerres.aacrjournals.org/content/suppl/2013/09/24/1078-0432.CCR-13-1425.DC1>

Cited articles This article cites 36 articles, 14 of which you can access for free at:
<http://clincancerres.aacrjournals.org/content/19/22/6305.full#ref-list-1>

Citing articles This article has been cited by 28 HighWire-hosted articles. Access the articles at:
<http://clincancerres.aacrjournals.org/content/19/22/6305.full#related-urls>

E-mail alerts [Sign up to receive free email-alerts](#) related to this article or journal.

Reprints and Subscriptions To order reprints of this article or to subscribe to the journal, contact the AACR Publications Department at pubs@aacr.org.

Permissions To request permission to re-use all or part of this article, use this link
<http://clincancerres.aacrjournals.org/content/19/22/6305>.
Click on "Request Permissions" which will take you to the Copyright Clearance Center's (CCC) Rightslink site.